A Method for Conducting Push-over Tsunami Analysis in Accordance with ASCE 7-16

A THESIS SUBMITTED TO THE GRADUATE DIVISION OF THE UNIVERSITY OF HAWAI‘I AT MĀNOA IN PARTIAL FULFILLMENT OF THE REQUIREMENTS FOR THE DEGREE OF

MASTER OF SCIENCE

IN

CIVIL ENGINEERING

May 2021

by

Derek William Aegerter

Committee:

Ian Robertson, Chair

Oceana Francis

DoSoo Moon

Acknowledgements

My greatest appreciation to:

Ian Robertson for his enthusiasm for teaching

Oceana Francis and DoSoo Moon for their support and instruction

Department of Civil Engineering Faculty and Staff for their flexibility during this pandemic

Gary Chock and Lyle Carden for their commitment to progress

Table of Contents

Table of Figures

Abstract

With the addition of Chapter 6 *Tsunami Loads and Effects* in ASCE 7-16 *Minimum Design Loads and Associated Criteria for Buildings and Other Structures,* significant analytical effort will soon be required of structural engineers to ensure that susceptible buildings are appropriately designed and detailed to withstand tsunami loads. ASCE 7-16 Chapter 6 offers a prescriptive approach to analyzing these loads and effects, which is intentionally conservative, while also allowing for alternative performance-based analysis. Research into performance-based non-linear analysis for tsunami loading has been conducted by Baiguera, et al. (2020) using the software *OpenSees*, however this software is primarily used in academia and is not particularly prevalent in the private sector of structural engineering. This study presents a procedure for performing a similar non-linear static pushover analysis for tsunami loading in accordance with ASCE 7-16 using *ETABS* software. This thesis establishes that the use of the procedure described herein can assist in targeted strengthening of a building which can reduce construction costs while adhering to the strength capacity requirements of Chapter 6 of ASCE 7-16.

Introduction

Several recent costly and deadly tsunamis including the 2004 Indian Ocean Tsunami, the 2010 Mentawai Tsunami, the 2011 Tohoku Tsunami, and others, have made evident the need for enhanced resilience of coastal communities to tsunami risks. It is expected that by improving the performance of critical facilities and tall buildings, susceptible communities can reduce the number of casualties, reduce the financial impact, and more rapidly recover after a tsunami. The addition of Chapter 6 *Tsunami Loads and Effects* in ASCE 7-16 *Minimum Design Loads and Associated*

Criteria for Buildings and Other Structures seeks to address the lack of guidance for tsunami prone areas.

The building and site locations used in this analysis are selected from McKamey (2019). The selection of the same building and locations, which were also used by Robertson (2020) and Baiguera et al. (2020), allow the results of this analysis to be compared with the analysis procedures described in those studies.

The two locations analyzed are Hilo, Hawaii, and Seaside, Oregon, shown in Figure 1 and Figure 2, respectively. Both selected locations are withing the Tsunami Design Zone (TDZ) where essential structures are required to be evaluated and wherein taller Tsunami Risk Category II (TRC) structures are strongly encouraged to be analyzed. This emphasis on taller TRC II buildings stems from the public perception that a vertical evacuation is an effective path even if the building is not specifically designated as a vertical evacuation structure. Many lives have been lost in previous tsunamis, such as the 2004 Sumatra–Andaman tsunami, due to tall building collapse with people who assumed they were safely evacuated. In Hawaii, both state and local governmental emergency management agencies recommend the practice of vertical evacuation in reinforced concrete and structural steel buildings over 100 feet in height.

Figure 1: Hilo Site. 19.720867 N 155.083286 W.

Figure 2: Seaside Site. 45.994743 N 123.929528 W.

The prototype building is a 6-story reinforced concrete structure with a ground floor height of 14 ft and 12 ft for each subsequent floor. The lateral force resisting system (LRFS) consists of Special Moment Resisting Frames (SMRFs) in both orthogonal directions. The building is considered to be Tsunami Risk Category II per the requirements of ASCE 7-16. The building overall is 254 feet wide by 86 feet deep and 74 feet tall as seen in Figure 3. Importantly, this building satisfies the seismic demand at both Hilo and Seaside, providing a reasonable example of a prototypical building in these areas.

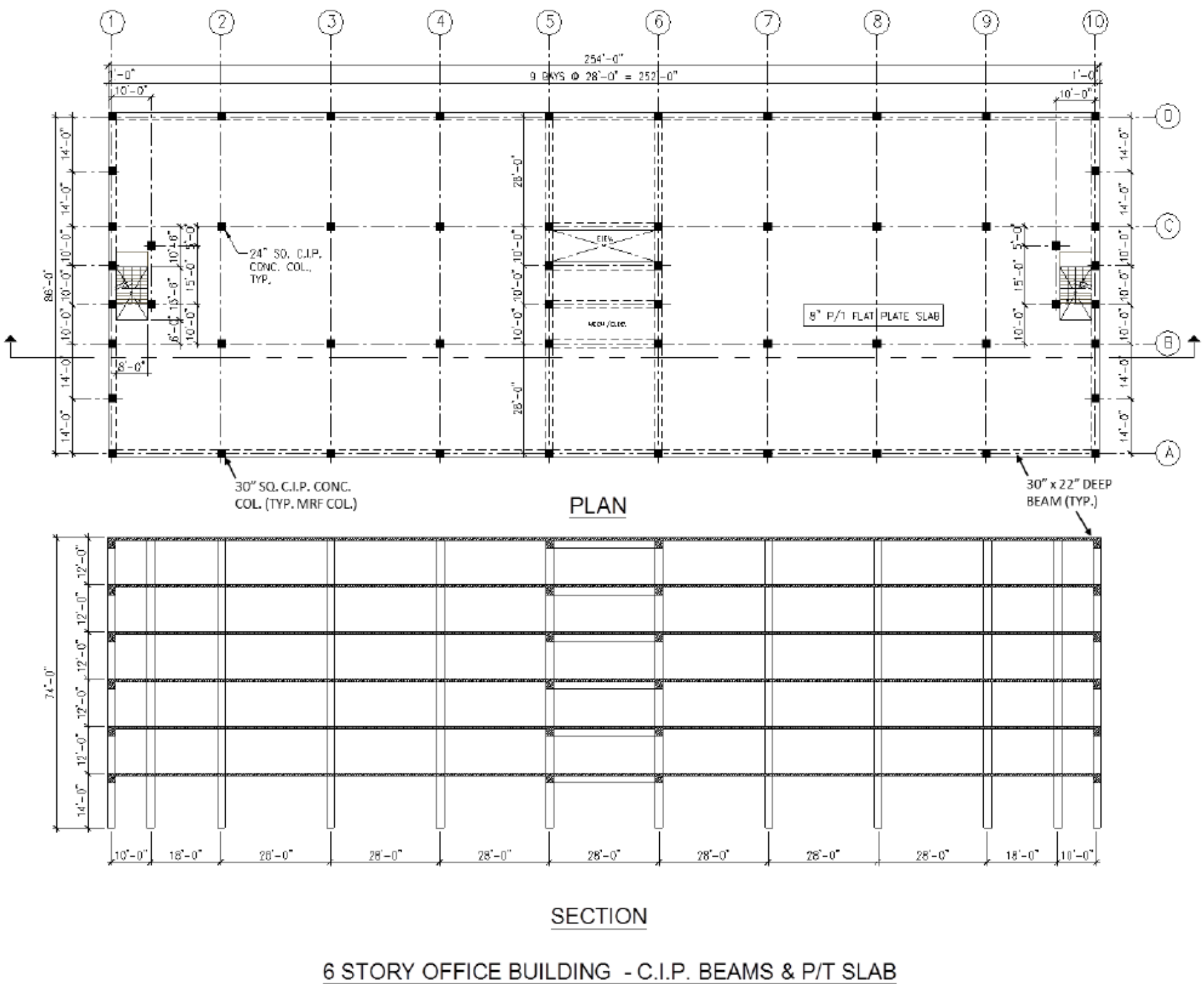

Figure 3: 6-Story Reinforced Concrete SMRF, after McKamey (2019)

Methods

Design Requirements

Section 6.8 of ASCE 7-16 prescribes the criteria which must be met for the Maximum Considered Tsunami (MCT) based on the building's Tsunami Risk Category. The building must be designed to meet Collapse Prevention Structural Performance criteria or better for the load combinations given by Equations 1 and 2. For this analysis, the foundation performance of the building is not considered and therefore H_{TSU} is ignored.

$$0.9D + F_{TSU} + H_{TSU} \qquad \textit{Eq. 1}$$

$$1.2D + F_{TSU} + 0.5L + 0.2S + H_{TSU} \qquad \textit{Eq. 2}$$

where,

F_{TSU} = tsunami load effect for incoming and receding directions of flow, and

H_{TSU} = load caused by tsunami-induced lateral foundation pressures developed under submerged conditions. Where the net effect of H_{TSU} counteracts the principal load effect, the load factor for H_{TSU} shall be 0.9.

Given that the buildings at both the Hilo and Seaside sites are classified as Seismic Design Category D, it is therefore permitted to use the following equation for determining Life Safety Structural Performance of the LFRS:

$$F_{TSU} < 0.75\Omega_0 E_{mh} \qquad \textit{Eq. 3}$$

where Ω_0 is the seismic overstrength factor and E_{mh} is the horizontal seismic load effect as determined by Chapter 12 of ASCE 7-16, and

$$F_{TSU} = \frac{1}{2}\rho_s I_{tsu} C_d b(h_e u^2) \qquad \textit{Eq. 4}$$

This F_{TSU} is maximum at the point of maximum flow velocity, defined as Load Case 2, LC2, shown in Figure 4. This maximum F_{TSU} will be referred to as $F_{T,LC2}$. It will be shown subsequently in this section that a significant amount of this force is transmitted directly into the foundation of the building and therefore not resisted by the LFRS. The remaining force which must be resisted by the LFRS will be referred to as $F_{T,net,LC2}$, in keeping with the convention followed by Baiguera et al. (2020).

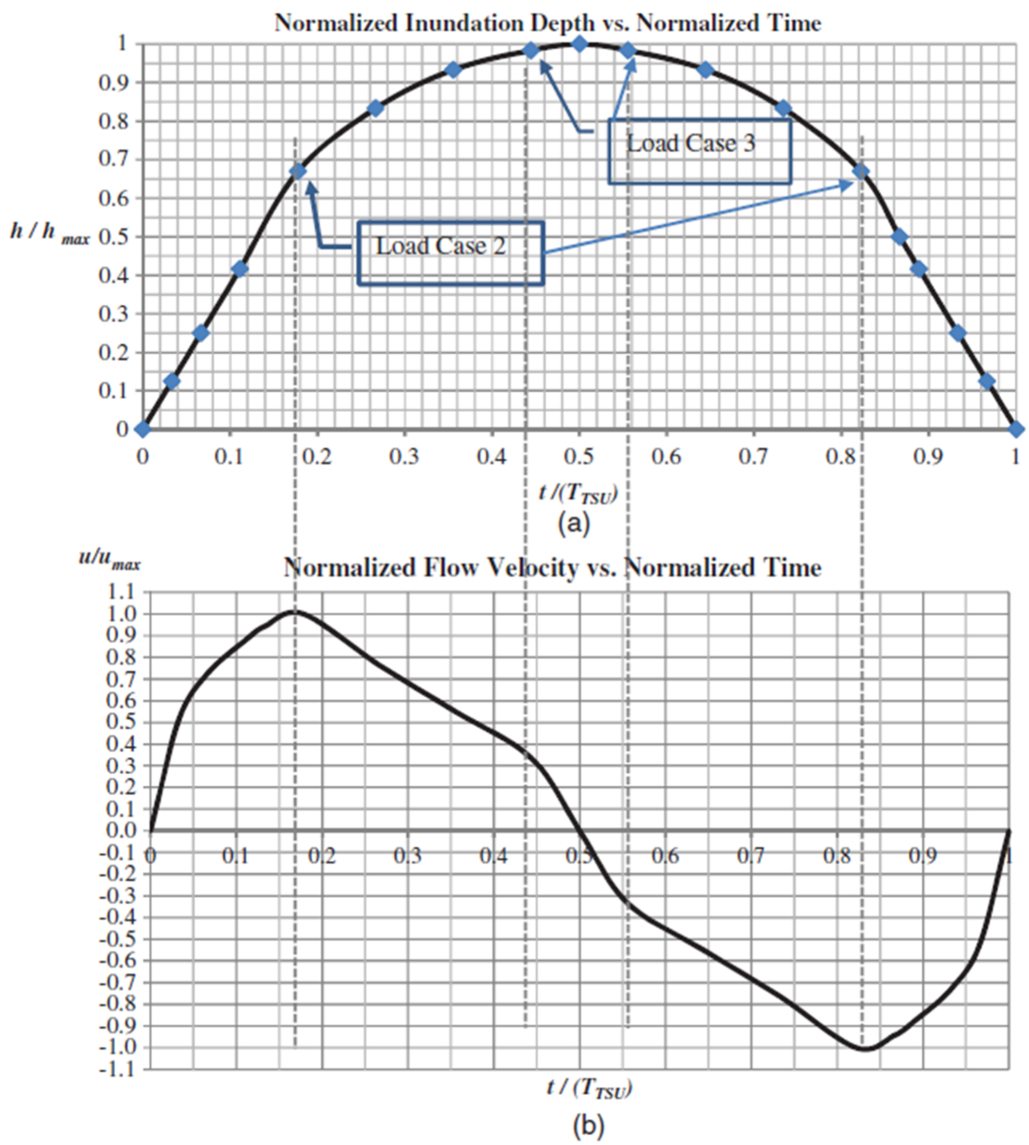

Figure 4: After ASCE (2017a), normalized flow velocity and depth vs. time.

Tsunami Risk Evaluation

The first step in performing the analysis is to determine the MCT flow parameters at the desired site location by performing an Energy Grade Line Analysis (EGLA) to determine design inundation depth and flow velocity. ASCE (2016) provides access to much of the requisite site information via their online design tool if the site in question is in Alaska, Hawai‘i, or along the west coast of the contiguous United States. The user is prompted to input the desired location based on address, coordinates, or map click. Next, transects can be drawn between the shore and the maximum runup elevation, as seen in Figure 5. The first transect, here labeled *0*, is drawn perpendicular to the shoreline as averaged 500 ft in either direction. The next two transects, here labeled *CW* and *CCW*, are drawn at ±22.5° from the first transect. These transects are all used to perform the EGLA and determine directionality of flow with respect to the building. While drawing transects, it is valuable to also draw corresponding bathymetric transects which will be used for tsunami bore risk assessment, seen in Figure 6.

For bore assessment, as many transects as possible should be drawn (up to three). Only two transects are sensible for the Hilo site, as the associated *CCW* transect is over land. ASCE 7-16, 6.6.4, states that “tsunami bores shall be considered where any of the following conditions exist:

1. The prevailing nearshore bathymetric slope is 1⁄100 or milder,
2. Shallow fringing reefs or other similar step discontinuities in nearshore bathymetric slope occur,
3. Where historically documented,
4. As described in the recognized literature, or
5. As determined by a site-specific inundation analysis.”

Figure 7 illustrates the bathymetric profiles for the two transects along with the described 1/100 slope. Overall, the average slope would appear to be *greater* than 1/100 out to a depth of 328 ft (100 m), however, along with a known history of tsunami bore in the area, it is obvious that a step discontinuity occurs due to a fringing reef at around 10,000 ft from shore which would require tsunami bore to be considered. Figure 7 is the plot of the two transects compared to a 1/100 slope.

Probabilistic earthquake-induced regional ground subsidence associated with a maximum considered tsunami caused by a local subduction earthquake must be considered when determining maximum inundation depth. No probabilistic data are available for the Hilo site. However, relative sea level change in Hilo is predicted to be 2.46 ft by the intermediate 2070 scenario of the NOAA Office for Coastal Management Sea Level Rise study (2017) and this change in sea level elevation must be considered when performing the Energy Grade Line Analysis (EGLA).

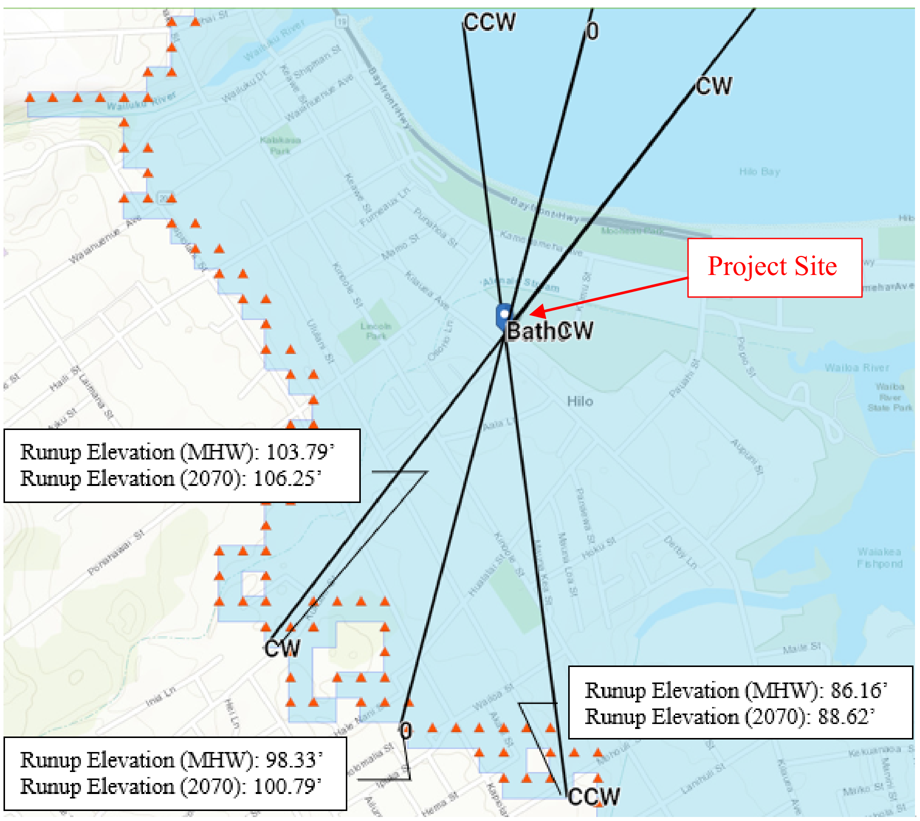

Figure 5. Transects used for EGLA for Hilo

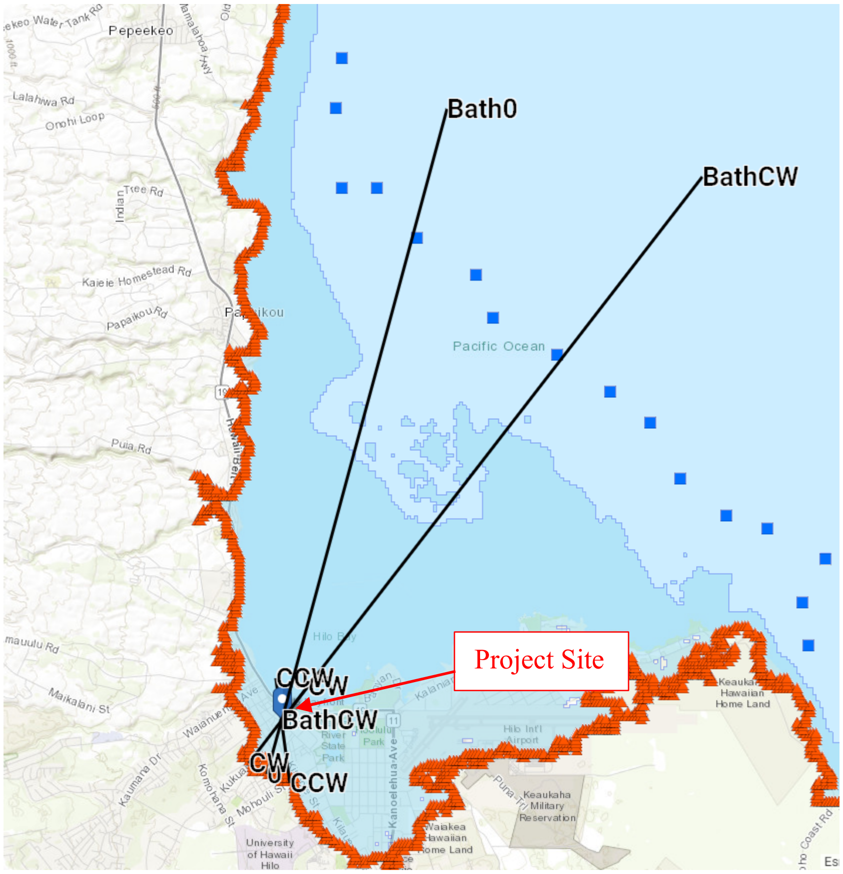

Figure 6. Transects used to determine nearshore bathymetry for Hilo

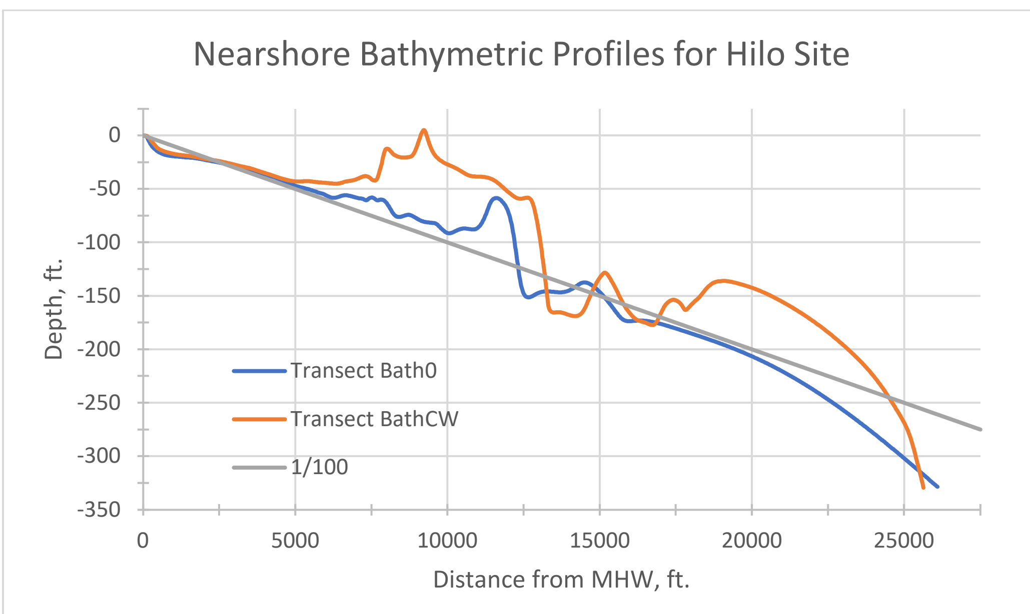

Figure 7. Nearshore Bathymetric Profiles for Hilo Site

The data from these transects can then be used to evaluate equations 6.6-1, 6.6-2, and 6.6-3 of ASCE 7 (Figure 8) using Excel or any other similar software. The analysis is performed from the point of maximum runup, where $E_{g,i} = 0$, back to the site location. The analysis provides the maximum flow velocity, u_{max}, and the maximum inundation depth, h_{max}, at each point, i. It is important to remember that the maximum flow velocity and inundation depths do not occur simultaneously. In order to avoid calculation errors, the value of h at the runup point should be set to $h \neq 0$. For this analysis, h was set at 0.001 ft., but the specific value does not significantly affect the results of the analysis. Figure 9 is a graphical representation of the output of the EGLA for the Hilo site, tabulated in Table 1.

$$E_{g,i} = E_{g,i-1} + (\varphi_i + s_i)\Delta x_i \qquad (6.6\text{-}1)$$

where

$E_{g,i}$ = Hydraulic head at point $i = h_i + u_i^2/2g = h_i(1 + 0.5F_{ri}^2)$;
h_i = Inundation depth at point i;
u_i = Maximum flow velocity at point i;
φ_i = Average ground slope between points i and $i-1$;
F_{ri} = Froude number = $u/(gh)^{1/2}$ at point i;
$\Delta x_i = x_{i-1} - x_i$, the increment of horizontal distance, which shall not be coarser than 100 ft (30.5 m) spacing;
x_i = Horizontal distance inland from NAVD 88 shoreline at point i; and
s_i = Friction slope of the energy grade line between points i and $i-1$, is calculated per Eq. (6.6-2).

$$s_i = (u_i)^2/((1.49/n)^2 h_i^{4/3}) = gF_{ri}^2/((1.49/n)^2 h_i^{1/3}) \qquad (6.6\text{-}2)$$

$$s_i = (u_i)^2/((1.00/n)^2 h_i^{4/3}) = gF_{ri}^2/((1.00/n)^2 h_i^{1/3}) \qquad (6.6\text{-}2.\text{si})$$

where

n = Manning's coefficient of the terrain segment being analyzed, according to Table 6.6-1, and
E_R = Hydraulic head of zero at the point of runup

Velocity shall be determined as a function of inundation depth, in accordance with the prescribed value of the Froude number calculated according to Eq. (6.6-3).

$$F_r = \alpha\left(1 - \frac{x}{x_R}\right)^{0.5} \qquad (6.6\text{-}3)$$

Figure 8: EGLA Equations from ASCE 7-16

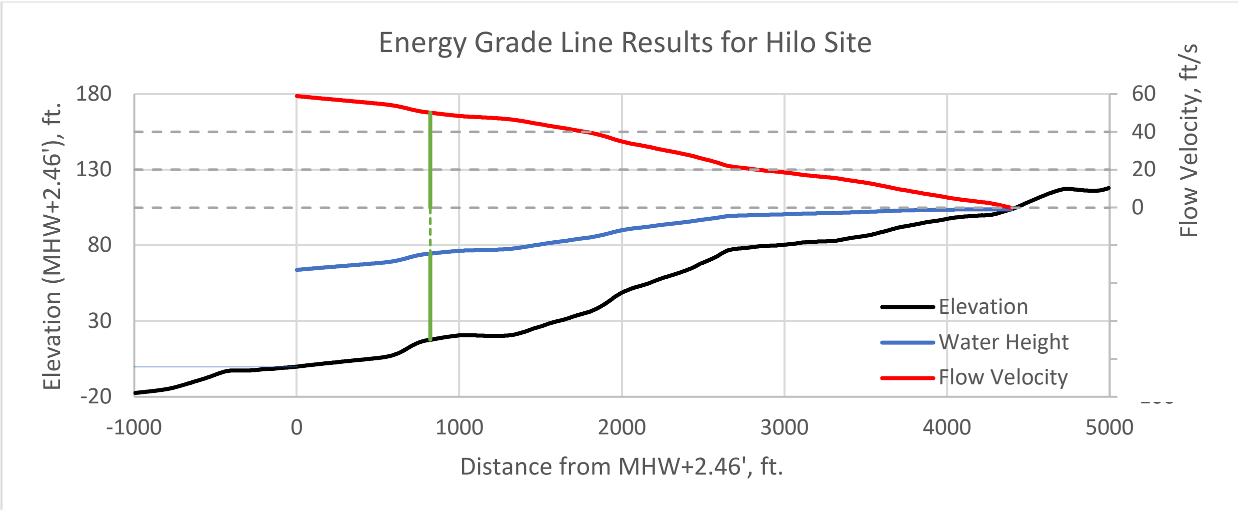

Figure 9: Results of EGLA for the Hilo Site

Table 1: Results of EGLA for Hilo Site and Associated Load Cases

	Inundation Depth, ft.	Flow Velocity, ft/s
No SLR, Max	56.7	48.6
2.46’ SLR, Max	57.0	50.2
Load Case 2	38.0	50.2
Load Case 3	57.0	16.7

Loading Assumptions

To ensure plastic hinges form in the order they would most likely form under actual tsunami conditions, the load distributions and sequences need to be properly determined. It is assumed that for all inundations depths that the total F_{TSU} is equally distributed across the entire face of the building up to the inundation depth. Referring back to Figure 4, it is also evident that for $0 < t < t_{LC2}$, F_{TSU} is always increasing because both flow velocity and inundation depth are always increasing for that time interval. For example, the analysis of the tsunami load as compared to the transient depth of the tsunami is seen in Figure 10. At an inundation depth of 38’, the rate of inundation slows and the velocity begins to decrease. This decrease in velocity results in reduced load on the structure.

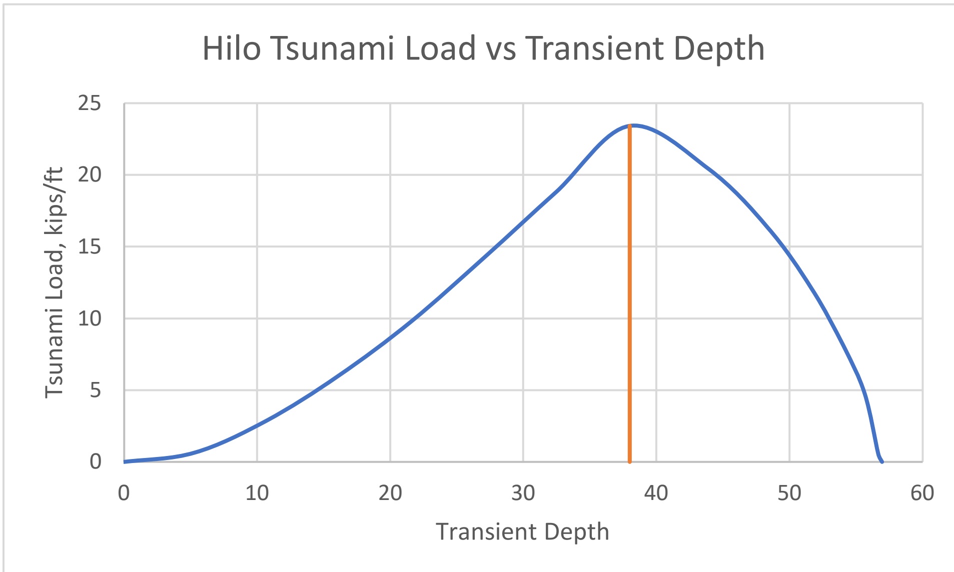

Figure 10: Tsunami Load for 0 < t < 0.5T

The proposed method for analyzing the LFRS involves applying an equivalent monotonically increasing point load at each storey diaphragm with tsunami pressures aggregated over each level’s tributary height. Because this check is only for the LFRS, the loads will be applied concentrically about the center of rigidity. These loads will be applied sequentially up the building, only after the previous storey has been fully loaded for the relative tsunami depth. In *ETABS*, this can be modeled using a series of nonlinear static pushover Load Cases which add upon the previous loads. To avoid confusion between *ETABS* and ASCE use of the term “Load Case,” “*ETABS* Load Case” will be referred to as ELC. Each nonlinear static pushover ELC will begin with the referenced Load Patterns having a magnitude of 0. The ELC will then incrementally increase the magnitudes of all selected Load Patterns proportionally to each other, checking for nonlinearity in the structure, until the full load is reached or until convergence issues arise. The stresses, deflections, and hinges can then all be carried over to the beginning of the next ELC.

The tsunami loads should be discretized into no fewer than one ELC per inundated storey, and care should be taken to ensure that each storey is loaded with approximately its maximum expected force prior to the next higher storey experiencing load which occurs where the inundation depth is halfway between the two storeys. It is expected that this will allow plastic hinges to develop in the appropriate order of occurance. Figure 11 shows the Hilo site discretized into seven steps. The distibuted tsunami load is show along with the lumped forces at each storey level. It is apparent that the bottom half of the ground floor distributed load is passed directly to the foundation, and therefore does not need to be accounted for in the LFRS strength.

The method used in this analysis does not require that each of the seven discretizations shown in Figure 11 be modeled as separate ELCs in *ETABS*. Rather, it is sufficient to model only the conditions where the load at the highest inundated storey is a maximum prior to the next storey experiencing load. This is because *ETABS* will proportionally increase all loads in a given ELC from 0 to their maximum value. For the Hilo, site this results in three ELCs derived from discretization steps 4, 6, and 7. Discretization steps 4 and 6 both have a small amount of tributary load at the next higher storey which will be ignored for the ELC. The ELC maximum storey loads for the Hilo site are listed in Table 2.

Table 2: Total Loads for each ELC, kips.

Storey	ELC 1	ELC 2	ELC 3
Fourth Floor	0	0	3694
Third Floor	0	6961	7403
Second Floor	5912	7541	8020

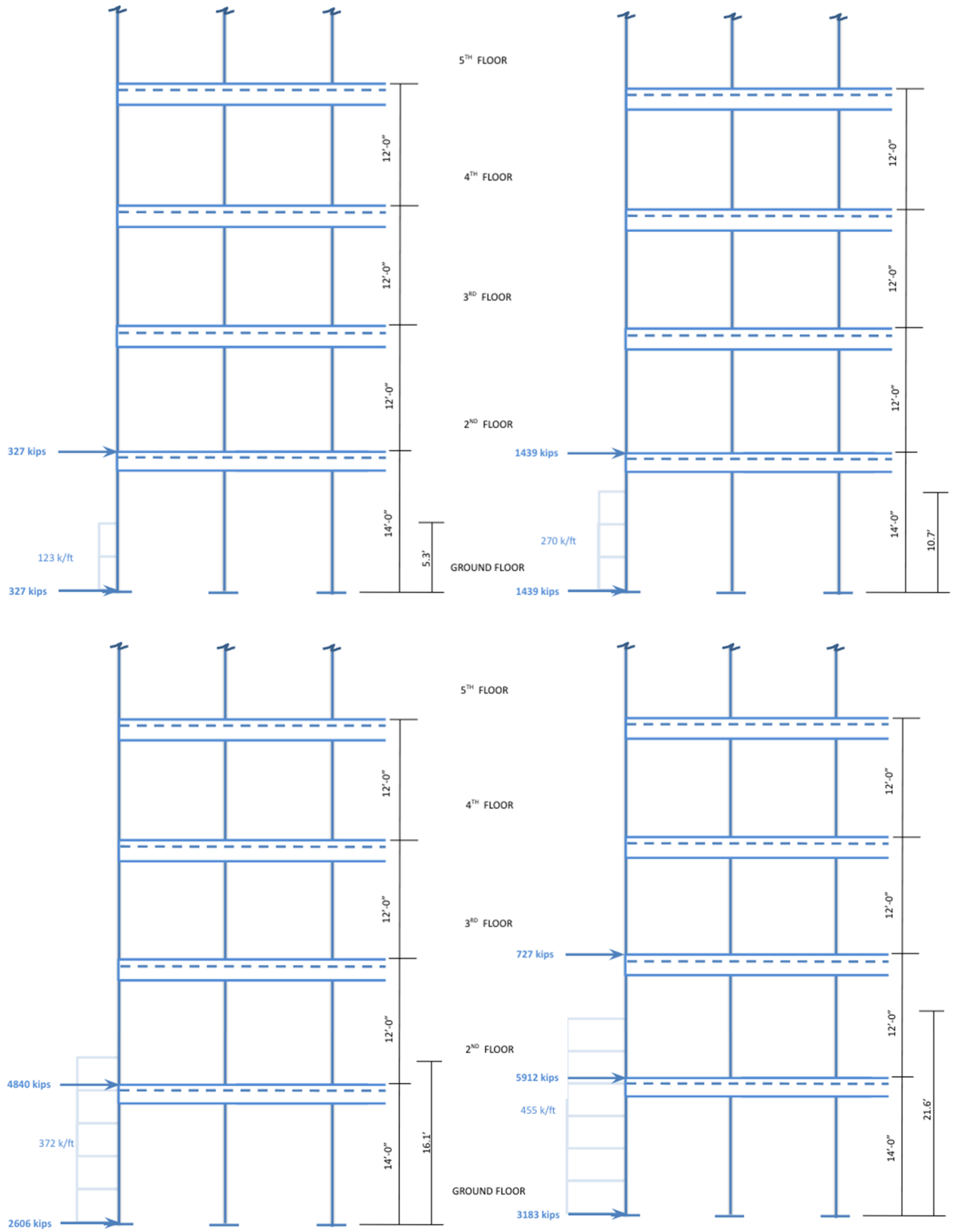

Figure 11: Discretization Steps – Hilo Site

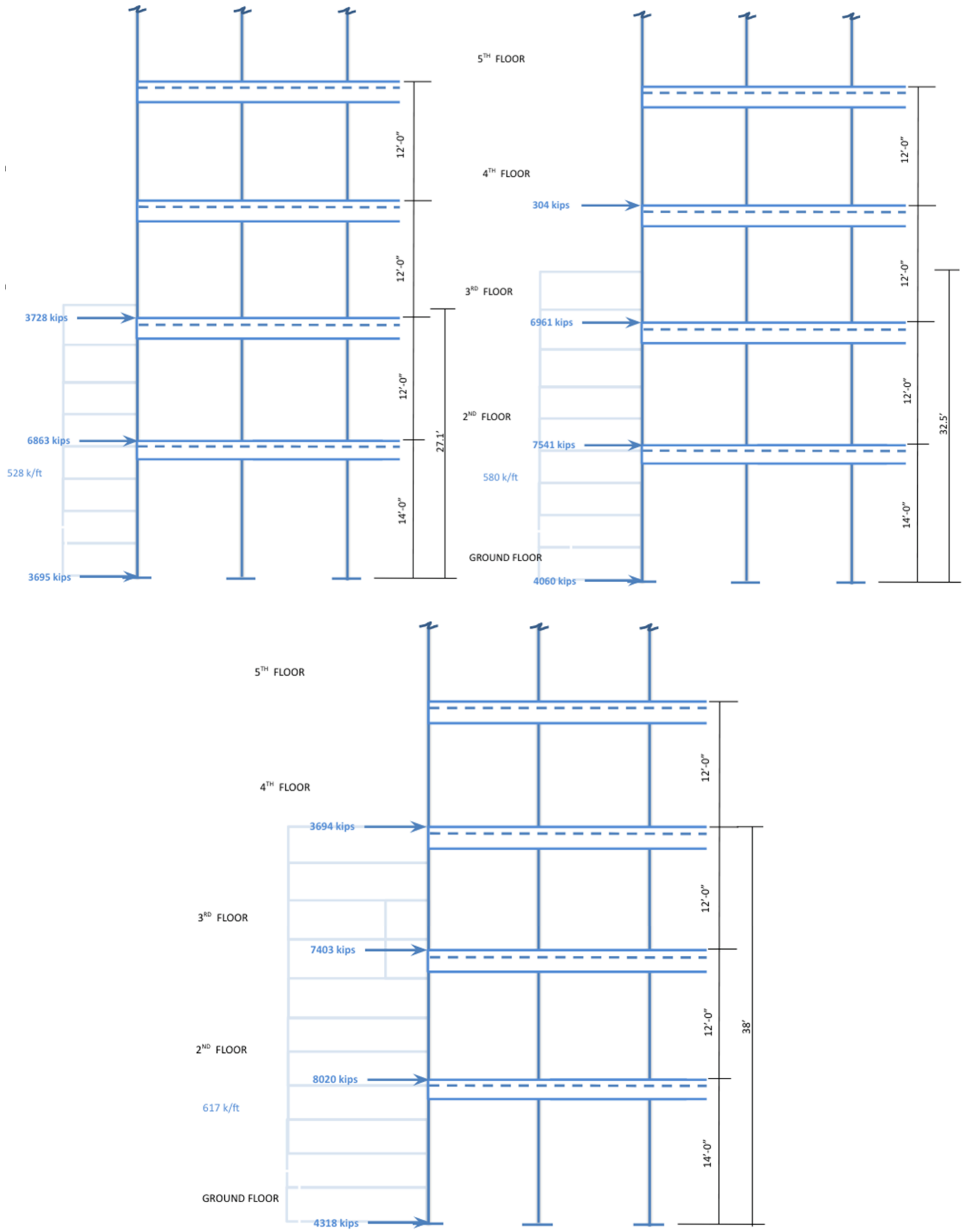

Figure 11, cont.: Discretization Steps - Hilo Site

Computational Analysis using *ETABS*

After MCT forces have been determined for LC2, a building model can be analyzed using a two-phase approach in *ETABS* which is similar to the ASCE-VDPO2 structural analysis method presented in Baiguera et al. (2020)

Building Model and Properties

The building model should be constructed in *ETABS* in a manner consistent with traditional pushover analysis. In this analysis, the buildings are assumed to have already been designed for the local seismic forces, as is the situation with much of the existing building stock in these locations. Therefore, the reinforced concrete beams and columns have been detailed in the *ETABS* model as required for the expected seismic loads. Additionally, because only the LFRS is being analyzed, we can model the storey diaphragms as rigid and massless. It is, however, important to account for the axial load on the columns due to the factored dead and live loads, as appropriate, so these loads must be added to account for massless diaphragms. The loads from the floors contribute to both the column strengths as well as P-delta effects.

Plastic hinges should be assigned to all column and beam segments up to at least the maximum inundation depth. The hinges in this analysis are defined within *ETABS* as interacting P-M2-M3 so that the axial force and moments are considered simultaneously. The hinges are then assigned to 0.1 and 0.9 relative length of each member at each storey so that a hinge can form at either end of the member, or both.

Load Conditions

After the building model has been assembled and all associated properties have been defined and assigned, the *ETABS* Load Patterns can be defined. For this analysis, one Load Pattern is required for each ELC – 3 for Hilo and 2 for Seaside. Additionally a Live Load Pattern and Dead Load Pattern, with self weight multiplier of 1, are required.

The mass source for the analysis needs to be set to appropriately compute axial column loads and P-delta effects. The mass source should include element self mass, and additional mass from speficied Load Patterns: Dead with a multiplier of 1, and Live with a multipler of 0.25. Mass source should include both vertical and lateral mass, lumped at storey levels. P-delta is defined for this analysis in ETBAS as “Non-Iterative – Based on Mass”.

ETABS automatically creates an ELC for each Load Pattern which must be properly defined. The Live Load ELC will remain the default Linear Static, but all other ELCs will need to be redefined as Nonlinear Static. The Seaside site will require two additional ELCs, which will be named TSU1 and TSU2.

Dead Load ELC

- The Dead Load ELC should be set to Nonlinear Static, as it will set the base case for all subsequent ELCs.
- The Mass Source should be set to the previously defined mass source (default name MsSrc1).
- Zero Initial Conditions. This setting will allow the entire series of nonlinear pushovers to be initialized with the Dead Load ELC.
- The applicable load pattern is Dead Load with a multiplier of 1.

TSU1

- TSU1 should be set to Nonlinear Static.
- The Mass Source should be set to the previously defined mass source (default name MsSrc1).
- Initial Conditions for the ELC should be set to "Continue from state at end of nonlinear case (Loads at End of Case ARE Included)"
    - Dead Load ELC should be set as the initial conditions.
- The applicable load pattern is TSU1 with a multiplier of 1.
- All other settings can be left as default.

TSU2

- TSU2 should be set to Nonlinear Static.
- The Mass Source should be set to the previously defined mass source (default name MsSrc1).
- Initial Conditions for the ELC should be set to "Continue from state at end of nonlinear case (Loads at End of Case ARE Included)"
    - TSU1 ELC should be set as the initial conditions.
- The applicable load pattern is TSU2 with a multiplier of 1.
- Load Application should be set to Displacement Control
    - Top drift used in this analysis is 2% which is 6.5 in.
    - Top Story is used moniter displacement in the direction of loading with a multiplier of 1.
- All other settings can be left as default.

Initially, a building can be analyzed using "Full Load" analysis in each ELC. If F_{TSU} exceeds the building capacity, then convergence issues will prevent the analysis from completing. The user will then need to determine which ELC causes the non-convergence and modify the it to be Displacement Control.

Loads

As previously explained and presented in Table 2, the loads for each ELC need to sum to the total expected force for each storey. Each nonlinear static ELC continues from the previous ELC with loads carrying over. Therefore, the loads applied in each ELC need to be decreased by the total amount previously applied to that storey. Continuing with the Hilo site example, the loads for each ELC are shown in Table 3.

Table 3: ***ETABS*** **Loads for each ELC, kips.**

Storey	ELC 1	ELC 2	ELC 3
Fourth Floor	0	0	3694
Third Floor	0	6961	7403 -6961 442
Second Floor	5912	7541 -5912 1629	8020 -7541 479

Results

Analysis for the Seaside site is presented in this analysis as it affords the most direct comparison with Baiguera *et al.* Upon initial analysis in *ETABS*, ELC TSU2 fails to converge and is therefore set to Displacement Control. The results of the analysis are shown in Figure 12 and are compared to the results of Baiguera *et al.* as well as the prescribed loads and strengths of $F_{T,net,LC2}$ and $0.75\Omega_0 E_{mh}$.

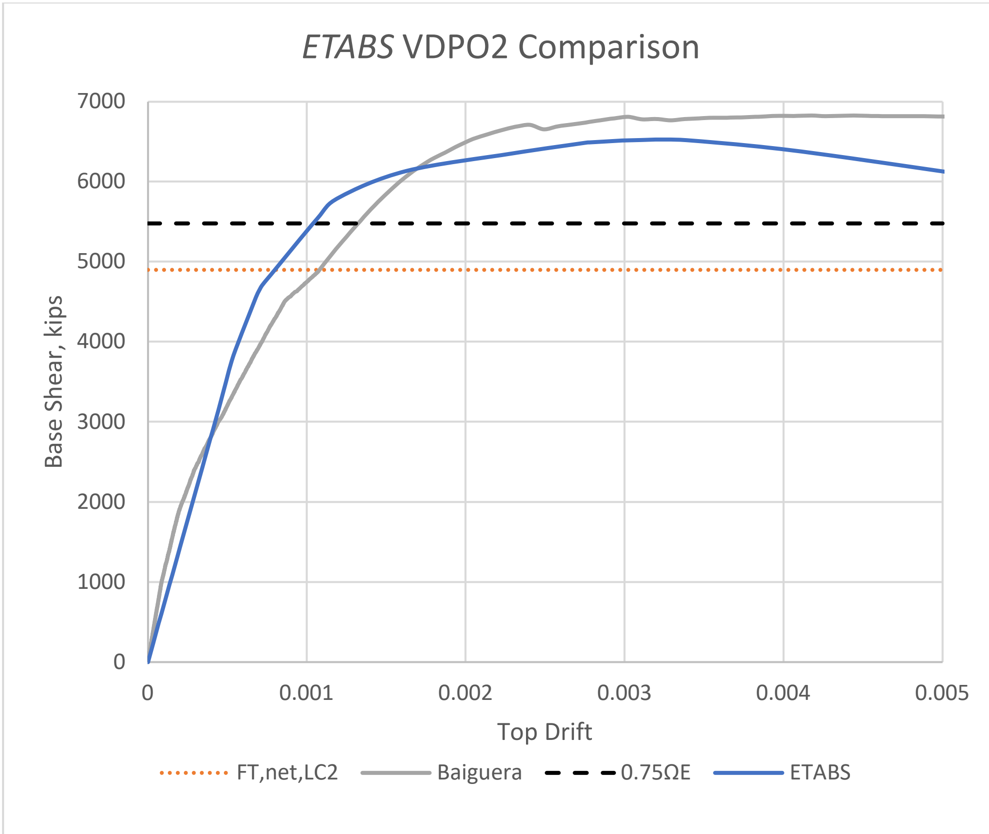

Figure 12: *ETABS* Analysis Output

Discussion

Strength of the building at Seaside exceeds the requirements of ASCE 7-16, even when only using the prescriptive approach as is evident by the fact that $0.75\Omega_0 E_{mh} > F_{T,net,LC2}$. However, the analysis by Baiguera *et al.* shows that in fact the building is nearly 25% stronger than the reduced seismic strength would suggest. The *ETABS* analysis similarly shows an approximately 20% increase in strength over ASCE 7-16 numbers. It is hypothesized that the lower strength of this analysis compared to Baiguera *et al.* is due in part to the fact that *OpenSees* uses a fiber-based plasticity model where this analysis utilized the lumped plasticity model of *ETABS* to keep analytical effort manageable. Fiber-based plasticity allows hinges to form continuously along the length of a member thereby accounting for increased ductility. Lumped plasticity, as used in this analysis, only allows for the formation of hinges at specific pre-defined locations and is a common conservative approach. However, fiber models require significantly more effort to construct the models as well as additional computing power.

Additionally, it can be seen in Figure 13 that special moment frames in the longitudinal direction are contributing to the transverse lateral resistance of the building because they are fixed at their base. This should be considered carefully for designers when choosing LFRS in each of the orthogonal direction and when modeling the building using this methodology.

It should be noted that this analysis does not include the modelling of shear hinges which may significantly affect the strength of the building. Also excluded from this analysis are foundation effects and component loading. Both of these effects are expected to also affect the overall strength of the building. Interestingly, even though beam hinges were included in the model, no plasticity was seen during the analysis. It is expected that the connections were designed to avoid Weak Column Strong Beam and it is therefore surprising that no hinges formed in these members.

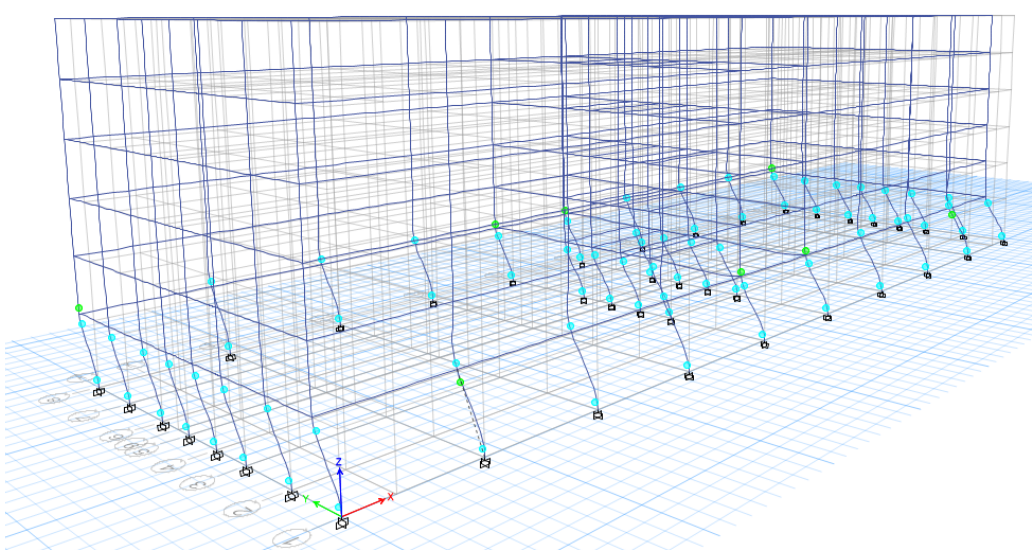

Figure 13: ***ETABS*** **Hinges**

Conclusion

The procedure described in this analysis allows increased accuracy when determining building strength against tsunami forces. This increased accuracy compared to Chapter 6 prescriptive approach of ASCE 7-16 can assist in the targeted strengthening of a building which will reduce construction costs while maintaining life-safety. Comparing the results of this analysis with that of other researchers, it is evident that this procedure is more conservative than other published approaches. This methodology provides a framework for engineering professionals to perform tsunami analysis using a relatively-common commercial software *ETABS*.

Additional research is needed to further assess the requirements of Chapter 6 of ASCE 7-16 as it applies to component-based strength, foundational tsunami effects, and shear strength. It is expected that a convenient addendum to this procedure can be developed to account for these effects.

References

ASCE (2016). *ASCE Tsunami Design Geodatabase.* https://asce7tsunami.online/

ASCE (2017a). *Minimum Design Loads and Associated Criteria for Buildings and Other Structures.* ASCE/SEI 7-16. Reston, VA, USA.

ASCE (2017b). *Seismic Evaluation and Retrofit of Existing Buildings.* ASCE/SEI 41-17, Reston, VA, USA.

Baiguera, M., Rossetto, T., Robertson, I., & Petrone, C. (2019). A Nonlinear Static Procedure for the Tsunami Design of a Reinforced Concrete Building to the ASCE7 Standard. *Proceedings of the SECED 2019 Conference*. SECED: London, UK.

Baiguera, M., Rossetto, T., Robertson, I., & Petrone, C. (2019). Towards a tsunami nonlinear static analysis procedure for the ASCE 7 standard. *Proceedings of the 2nd International Conference on Natural Hazards & Infrastructure 2019*. National Technical University of Athens: Chania, Greece.

Baiguera, M., Rossetto, T., Robertson, I., & Petrone, C. (2020). A Procedure for Performing Nonlinear Pushover Analysis for Tsunami Loading to ASCE7. *ASCE Journal of Structural Engineering.*

Chock, G. Y., Carden, L., Robertson, I. N., Wei, Y., Wilson, R., & Hooper, J. (2018). Tsunami-Resilient Building Design Considerations for Coastal Communities of Washington, Oregon, and California. *ASCE Journal of Structural Engineering*, *144*(8):04018116.

Leslie, Rahul. (2012, June). The Pushover Analysis in Its Simplicity. *Civil Engineering & Construction Review,* 118-126.

McKamey, J. (2019). *Cost Implications for Including Tsunami Design in Mid-Rise Buildings along the US Pacific Coast*. [Unpublished master's thesis]. University of Hawaiʻi at Mānoa.

NOAA. (2017, January). *Global and Regional Sea Level Rise Scenarios for the United States.* NOAA Technical Report NOS CO-OPS 083. https://tidesandcurrents.noaa.gov/publications/techrpt83_Global_and_Regional_SLR_Scenarios_for_the_US_final.pdf.

Robertson, I. N. (2020). *Tsunami Loads and Effects: Guide to the Tsunami Design Provisions of ASCE 7-16.* ASCE.